The Astrophysical Journal, 797:64 (9pp), 2014 December 10 doi:10.1088/0004-637X/797/1/64


# RELATIVE BRIGHTNESS OF THE $O^+(^2D–^2P)$ DOUBLETS IN LOW-ENERGY AURORAE

D. K. Whiter[1,2], B. S. Lanchester[2], B. Gustavsson[2,3], N. I. B. Jallo[2,4], O. Jokiaho[2], N. Ivchenko[5], and H. Dahlgren[2,5]
[1] Finnish Meteorological Institute, Erik Palménin Aukio 1, FI-00560 Helsinki, Finland; daniel.whiter@fmi.fi
[2] School of Physics & Astronomy, University of Southampton, SO17 1BJ, UK
[3] Department of Physics and Technology, University of Tromsø, NO-9011 Tromsø, Norway
[4] Physics Department, College of Science, University of Baghdad, Iraq
[5] Royal Institute of Technology (KTH), Teknikringen 31, SE-100 44 Stockholm, Sweden
*Received 2014 September 10; accepted 2014 October 20; published 2014 November 25*

## ABSTRACT

The ratio of the emission line doublets from $O^+$ at 732.0 nm ($I_{732}$) and 733.0 nm ($I_{733}$) has been measured in auroral conditions of low-energy electron precipitation from Svalbard (78°.20 north, 15°.83 east). Accurate determination of $R = I_{732}/I_{733}$ provides a powerful method for separating the density of the $O^+$ $^2P^o_{1/2,3/2}$ levels in modeling of the emissions from the doublets. A total of 383 spectra were included from the winter of 2003–2004. The value obtained is $R = I_{732}/I_{733} = 1.38 \pm 0.02$, which is higher than theoretical values for thermal equilibrium in fully ionized plasma, but is lower than reported measurements by other authors in similar auroral conditions. The continuity equations for the densities of the two levels are solved for different conditions, in order to estimate the possible variations of $R$. The results suggest that the production of ions in the two levels from O ($^3P_1$) and O ($^3P_2$) does not follow the statistical weights, unlike astrophysical calculations for plasmas in nebulae. The physics of auroral impact ionization may account for this difference, and therefore for the raised value of $R$. In addition, the auroral solution of the densities of the ions, and thus of the value of $R$, is sensitive to the temperature of the neutral atmosphere. Although the present work is a statistical study, it shows that it is necessary to determine whether there are significant variations in the ratio resulting from non-equilibrium conditions, from auroral energy deposition, large electric fields, and changes in temperature and composition.

*Key words:* atomic data – atomic processes – line: formation – planets and satellites: aurorae – solar–terrestrial relations

*Online-only material:* color figures

## 1. INTRODUCTION

Emissions from the metastable states of atomic oxygen are observed in the atmospheres of planets as aurorae and airglow, and also in astrophysical plasmas, such as gaseous nebulae. In particular, the emission line doublets from $O^+$ at 732.0 nm ($I_{732}$) and 733.0 nm ($I_{733}$) are the result of transitions from the two levels $2s^22p^3\ ^2P^o_{1/2,3/2}$ to $2s^22p^3\ ^2D^o_{5/2}$ and $2s^22p^3\ ^2D^o_{3/2}$, respectively. The ratio of the brightness of these two doublets, $R = I_{732}/I_{733}$, is of interest in both atmospheric and astrophysical studies. For example, it has been used in theoretical studies to determine the transition probabilities between the two states of the oxygen ion, and to study the electron quenching rates of the metastable states (Seaton & Osterbrock 1957; De Robertis et al. 1985; Zeippen 1987; Barnett & McKeith 1988; Keenan et al. 1999).

The doublets are observed in terrestrial airglow as a result of photoionization of atomic oxygen by solar UV with wavelengths less than 66.6 nm. Sharpee et al. (2004) presented the first nightglow observations of the doublets from the W. M. Keck Observatory on Hawaii, in which all four lines were resolved. In aurorae, the excited $O^+$ ions are produced by impact ionization from electrons. Modeling shows that the doublet emission lines in aurorae are most sensitive to electron precipitation of energy less than 200 eV, with an emission height maximum above 250 km. The emission is therefore a very useful indicator of low-energy precipitation, at times when the brightness is high. It is often stronger during times of distinctive rayed aurorae (Ivchenko et al. 2005; Semeter 2003) and can be used as a diagnostic of intense field-aligned currents, when low-energy precipitation is likely to be dominant.

In both airglow and aurorae, collisions of the excited $O^+$ ions with nitrogen molecules and oxygen atoms cause the ion to deactivate without radiating. The height dependent emission rates of the doublets have been used to calculate the quenching rates of the upper state (Rusch et al. 1977; Rees 1989; Chang et al. 1993; Stephan et al. 2003). More recently, direct optical observations of the 732.0 nm doublet were used for the first study of the decay time of the ions, using ionospheric modeling (Dahlgren et al. 2009). The same emissions were used to infer plasma velocities in discrete auroral features, by tracking the motion of the $O^+$ afterglow once production had ceased. One of the motivations of the present work is to increase the accuracy of 732.0 nm emission modeling to improve the quality of these velocity measurements, and hence infer the electric fields present in the auroral ionosphere at unprecedented temporal and spatial resolution. In the case of the $O^+$ doublets, the relative concentrations of the two emitting levels $^2P^o_{1/2}$ and $^2P^o_{3/2}$ are needed. The brightness ratio $R = I_{732}/I_{733}$ gives a method of obtaining this concentration ratio, as shown in the Appendix.

The only known auroral measurements of the brightness ratio are from Sivjee et al. (1979), who measured the $O^+$ doublets at 732.0 nm and 733.0 nm during a period of low-energy electron precipitation from Fairbanks, Alaska. They found a value of the ratio $R = I_{732}/I_{733}$ of $1.55 \pm 0.05$ compared with their calculated theoretical values of 1.23 (>270 km) and 1.31 (<220 km) assuming thermal equilibrium. In the present work, $R$ is determined from auroral spectrographic measurements from Svalbard, Norway, over one winter of near-continuous observations (2003 December–2004 January). The data have been selected for auroral events that are dominated by the $O^+$ doublets, and thus are from times of low-energy precipitation.

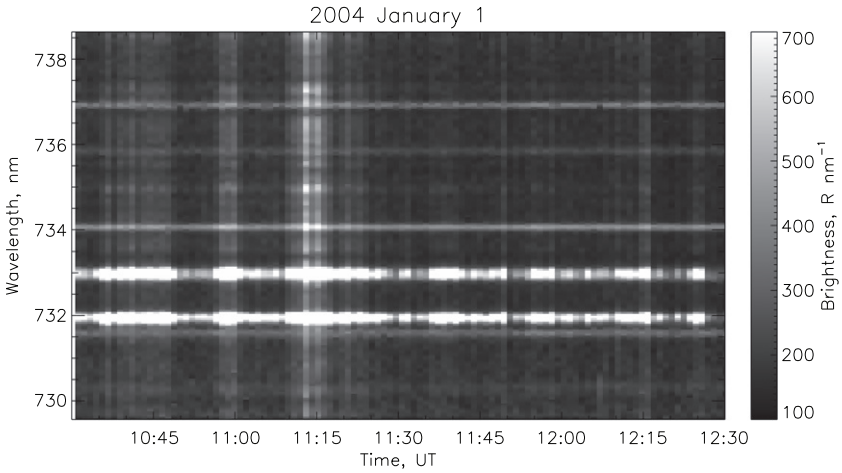


**Figure 1.** Example of spectra showing all emissions in wavelength range 730–738 nm.

The location of Svalbard is unique in that it has continuous dark hours throughout the winter months, so that during the hours around magnetic noon, the optical signatures of low-energy precipitation in the magnetospheric cusp are measured.

As noted by Slanger et al. (2011) in work on a different emission ratio from atomic oxygen, "agreement among theoreticians on the numerical value of a particular physical parameter must still withstand the test of observation." The observations presented here give values of the ratio $R = I_{732}/I_{733}$ which differ from theoretical values under certain assumptions. The assumptions and limitations of a theoretical treatment of the production and loss of $O^+(^2P^o)$ ions are considered. As highlighted in both Sivjee et al. (1979) and Sharpee et al. (2004), there are problems associated with measuring the low intensities of the doublets, and their separation from contaminating emissions, in particular OH lines, but also $N_2$ bands. The rigorous methods used to subtract these underlying emissions are described. This work provides a statistical estimate of $R$, its standard deviation, and significance; further, it is important to consider whether there is a natural variation in the ratio of the doublets associated with auroral conditions, which may affect the physical interpretation of the theory.

## 2. OBSERVATIONS AND ANALYSIS

The Spectrographic Imaging Facility (SIF) is a platform of instruments designed for detailed studies of the aurora, situated near Longyearbyen, Svalbard at geographic latitude 78°.20 north and longitude 15°.83 east. The main instrument is the High Throughput Imaging Echelle Spectrograph (HiTIES; Chakrabarti et al. 2001). Light from an 8° slit is collimated, diffracted by an echelle grating, and re-imaged on the detector. Overlapping diffraction orders are separated by a mosaic of interference filters. In these observations the FWHM instrument function gives maximum spectral resolution of $0.122 \pm 0.002$ nm. Typical integration times are 10–60 s. The spectra used in the present statistical analysis have been post-integrated to a time resolution of 120 s. The slit was aligned with the magnetic meridian and centered on the magnetic zenith.

Figure 1 is a sample of data on 2004 January 1 from the HiTIES $O^+$ panel between wavelengths 730.0 nm and 738.0 nm. Each exposure has been integrated in the spatial direction over 1° corresponding to the region closest to the magnetic zenith, and plotted as a time series of spectra. During this interval of 2 hr between 10:30 UT and 12:30 UT, the $O^+$ doublets at 732.0 nm and 733.0 nm are present throughout, as are several rotational lines from the airglow OH Meinel (8, 3) band. At 11:15 UT a clear event of more energetic precipitation occurs, so that the band structure from $N_2$ $1P(5, 3)$ emissions is seen across all wavelengths.

Figure 2 shows line spectra at three times with different dominant emissions. The top panel of Figure 2 is a sample spectrum from 2003 December 28 of the $N_2$ $1P(5, 3)$ band structure during a time of energetic precipitation. Such spectra are eliminated from the analysis. The middle panel of Figure 2 shows HiTIES spectra added between 21:10 UT and 21:40 UT on 2003 December 23. During this time the sky was clear and there was no aurora, allowing for accurate measurements of the OH line intensities. The most prominent lines in the region of the $O^+$ doublets are $P_1(2)$ at 731.6 nm, $P_2(3)$ at 732.9 nm, and $P_1(3)$ at 734.1 nm (Meinel 1950; Sivjee & Hamwey 1987), as shown by the shaded regions. The bottom panel is a typical spectrum of auroral emissions resulting from low-energy precipitation, integrated over 5 minutes. The $O^+$ doublets are clearly dominant at 732.0 nm and 733.0 nm. The OH lines are also present, as well as a background level of emission, which may contain a small contribution from the $N_2$ band. The 731.6 nm OH and 732.0 nm $O^+$ lines are resolved separately. However, the peak at 733.0 nm contains both the $O^+$ doublet and the $P_2(3)$ OH line.

The emission lines appear as approximately Gaussian-shaped peaks in the HiTIES spectra, as a result of the instrument function. In order to obtain the brightness (in Rayleighs) of each line, the measured spectrum is integrated within the wavelength range of each Gaussian peak and an appropriate background subtracted. Within the background emission that is discarded from all the peaks will be a variable contribution from the $N_2$ $1P(5, 3)$ band. In order to use only data from low-energy auroral events, the wavelength region between 736.5 nm and 737.5 nm, shown in hatched shading in the bottom panel of Figure 2, is used to select events where the "$N_2$ background" is less than a chosen percentage of the integrated brightness of both $O^+$ doublets. This wavelength region has no other known auroral emissions of significance.

In order to be certain that the contribution from $N_2$ has been removed correctly from the remaining spectra, synthetic $N_2$ $1P(5, 3)$ band emissions have been modeled as a function of rotational temperature, following the methods of Jokiaho et al. (2008, 2009). These synthetic spectra are then used

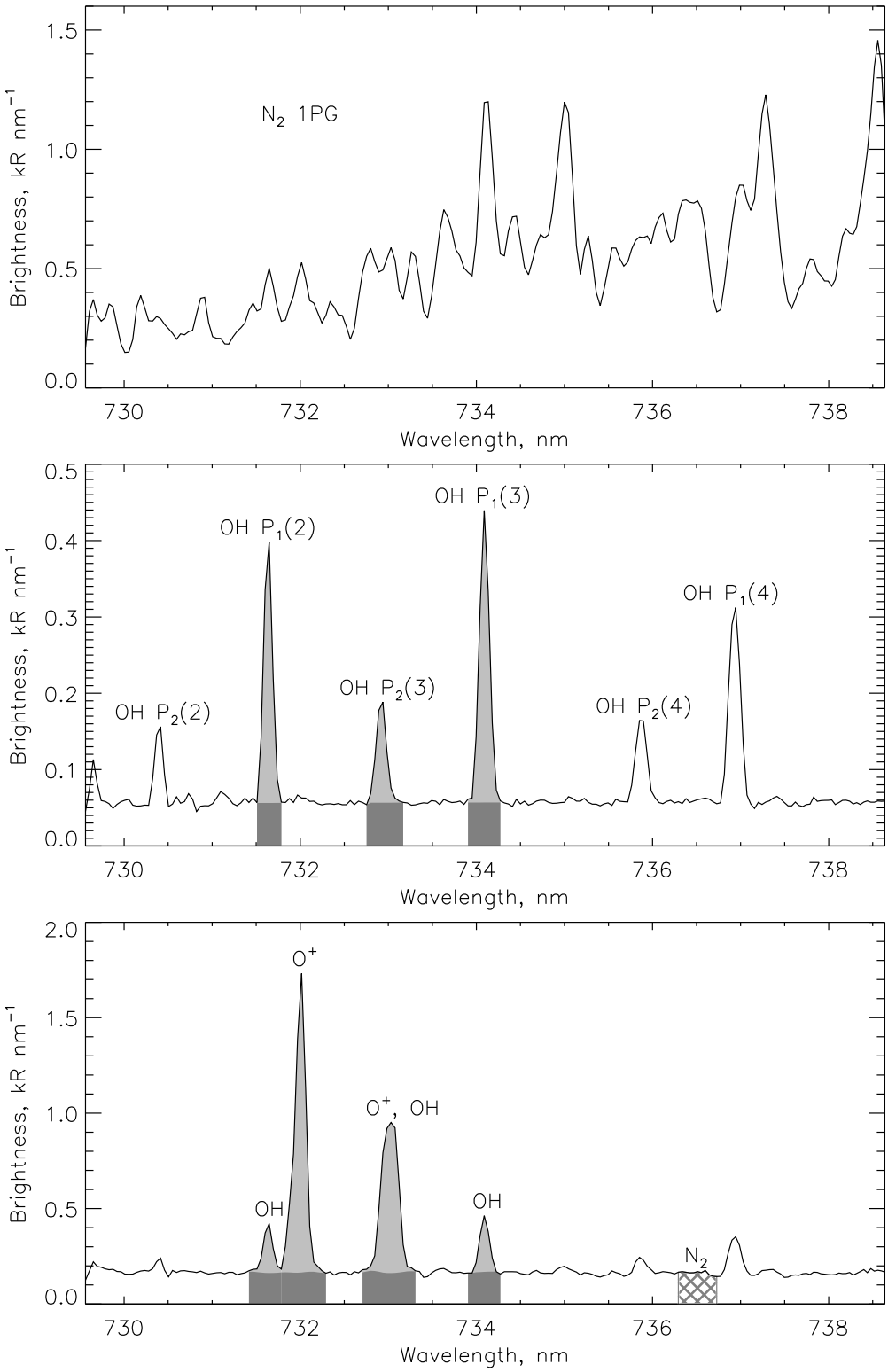


**Figure 2.** Top: spectrum dominated by $N_2$ band structure. Middle: HiTIES spectrum of purely OH integrated over 30 minutes. Bottom: typical spectrum from low-energy precipitation with both $O^+$ and OH, integrated over 5 minutes.

with a combination of nine Gaussian peaks, representing the four lines of the $O^+$ doublets and five OH lines ($P_1(2)$, $P_2(3)$, $P_1(3)$, $P_2(4)$, and $P_1(4)$), and a straight line for the continuum background, all of which are fitted to the measured spectra between 730.7 nm and 738.7 nm. The central wavelengths of the Gaussian peaks are fixed parameters in the fit, and are taken from Sharpee et al. (2004) and Phillips et al. (2004). The FWHM of the Gaussians is constrained to be identical for all peaks. Ratios between OH peaks which are independent of rotational temperature are fixed at theoretical values from Phillips et al. (2004), except for the $I(P_2(3))/I(P_1(3))$ ratio which comes from our observations (see below). In total the fit has 11 free parameters, and an iterative process is used to minimize the squares of the residuals between the fitted and the measured

**Table 1**
Previous Measured and Theoretical Values of the Ratio $R = I_{732}/I_{733}$

| Author | $R = I_{732}/I_{733}$ | Emission | Electron Density |
|---|---|---|---|
| Seaton & Osterbrock (1957) | 1.24 | Theory | Low |
| | 1.31 | Theory | High |
| Kaler et al. (1976) | 1.2 | Nebulae | |
| Sivjee et al. (1979) | $1.55 \pm 0.05$ | Aurora | |
| Sharpee et al. (2004) | 1.3 | Nightglow | |
| This work | $1.38 \pm 0.02$ | Aurora | |

spectra. The resulting background subtracted from each spectral line is shown in dark gray in Figure 2. The standard deviation of the residuals between the fitted and measured spectra gives an estimate for the random uncertainty associated with each pixel measurement within the spectrum, and is used to calculate the random uncertainty associated with each emission line brightness.

In order to remove the 732.9 nm OH emission from the 733.0 nm doublet, the strong emission at 734.1 nm is used. The corrected brightness of $O^+$ at 733.0 nm, $I_{733}$, is obtained from:

$$I_{733} = I_{733}^{\rm obs} - I_{734}^{\rm obs}\,\rho_1, \quad (1)$$

where $I_{733}^{\rm obs}$ and $I_{734}^{\rm obs}$ are the measured brightnesses of the lines at 733.0 nm and 734.1 nm, respectively, with the background subtracted, and $\rho_1 = I(P_2(3))/I(P_1(3))$ is the ratio of OH line brightnesses from the clear sky period in the middle panel of Figure 2.

The histogram in the top panel of Figure 3 shows the daily distribution of spectra between 2003 December 22 and 2004 January 3 that meet the criterion for low-energy electron precipitation (383 spectra). The mean ratio $R = I_{732}/I_{733}$ for each 24 hr period is shown as a horizontal dashed bar above the histogram, with its value given on the right hand ordinate. A probability density function for the ratio is computed by kernel density estimation, and is shown as gray shading to indicate the distribution of the ratio values obtained each day. The mean value of $R = 1.38 \pm 0.02$ is plotted as a horizontal line, but it is barely visible due to the closeness of the distributions to the mean value throughout. The uncertainty quoted here is the standard deviation of the measured $R$-values. In the middle panel of Figure 3 all values of $R$ for this season are plotted against the measured brightness of the 732.0 nm doublet, showing that the ratio is independent of brightness. The bottom panel shows all values of $R$ plotted against time of day in UT. Most data points are from the time spanning magnetic noon (09:15 UT). There is no observable trend with time of day, nor any substantial effect from a particular day's data (see discussion below, and the online color version of the figure).

## 3. FACTORS AFFECTING RATIO

The measured values of $R$ reported here are higher than measurements in nebulae and theoretical estimates (see Table 1). The important question to be answered is whether there are physical explanations for the difference. It is necessary to estimate what factors might affect $R$, in particular under auroral conditions in the collision-dominated ionosphere, which could be very different from those in gaseous nebulae, or even nightglow.

In gaseous nebulae, $O^+$ ions are excited from the $^4S^o$ ground state of the ion to the two levels of the $O^+(^2P^o)$ state by collisions with thermal electrons. Thus the relative strengths

**Table 2**
$O^+$ Transitions

| Transition | Wavelength (nm) | Einstein Coefficient ($s^{-1}$) |
|---|---|---|
| $^2D^o_{5/2}$–$^2P^o_{1/2}$ | 731.904 | $5.63 \times 10^{-2}$ |
| $^2D^o_{5/2}$–$^2P^o_{3/2}$ | 732.012 | $1.07 \times 10^{-1}$ |
| $^2D^o_{3/2}$–$^2P^o_{1/2}$ | 732.968 | $9.39 \times 10^{-2}$ |
| $^2D^o_{3/2}$–$^2P^o_{3/2}$ | 733.076 | $5.78 \times 10^{-2}$ |

**Note.** Wavelengths from Sharpee et al. (2004), Einstein coefficients from Zeippen (1987).

of the resulting emissions can be related to the density and temperature of the electrons in the plasma. However, for the limit of high densities, collisional deactivation plays an important role, so that there is a balance between collisional excitation and deactivation. For low densities, collisional deactivation is negligible, and the population of the upper levels is given by the equilibrium between the rate of radiation from the levels and collisional excitation of the levels. At intermediate densities, observed ratios of two or more pairs of lines have been used to estimate the density and temperature of the electron gas (De Robertis et al. 1985; Barnett & McKeith 1988; Keenan et al. 1999). Theoretical values of $R$ are given by De Robertis et al. (1985), which are in agreement with those of Seaton & Osterbrock (1957), varying between 1.24 for a low-density regime ($N_e < 10^3$ cm$^{-3}$) and 1.31 for a high-density regime ($N_e = 10^8$ cm$^{-3}$), both for $T_e = 10^4$ K.

In Earth's high-latitude ionosphere the $O^+(^2P^o)$ state is produced by energetic electron impact on atomic oxygen through

$$e^- + O(^3P) \rightarrow 2e^- + O^+(^4S^o,\ ^4D^o,\ ^2P^o)$$

where approximately 20% of the ionization leads to the $^2P^o$ state (Rees et al. 1982; Dalgarno & Lejeune 1971). The results of Sivjee et al. (1979) are the only auroral measurements similar to those presented here, having been measured during a short period of low-energy electron precipitation. In trying to explain their high ratio of $1.55 \pm 0.05$ they considered the effect of errors in the transition probabilities, uncertainties in the quenching rates, and the effect of assuming that the population of the two levels of the upper state were proportional to their statistical weights. They also discussed the effect of variations in the relative populations of the levels of the O atom ($^3P_1$ and $^3P_2$) from which the excited ion is produced in aurorae and airglow. They concluded that the most plausible reason for the discrepancy between their measured and theoretical ratio was a 9% error in the values of the Einstein coefficients, but did not rule out the other factors. They did not consider background contamination from either OH or $N_2$ to be a factor.

In other terrestrial measurements, but in airglow and not aurorae, Sharpee et al. (2004) found a value of $R = 1.3$, which they claim agreed with the high-density theoretical value for thermally populated $^2P^o$ levels and inferred that the $O^+(^2P^o)$ level populations are in thermal equilibrium at the height of the nightglow emission. They assumed therefore that the relative line brightness of the doublets depended on the statistical weights and the spontaneous transition probabilities, thus providing a check on the values of the Einstein coefficients used. They recalculated the ratio $R$ from the equations of Sivjee et al. (1979) using updated Einstein coefficients, and found little change to the high-density theoretical ratio. Table 2 gives

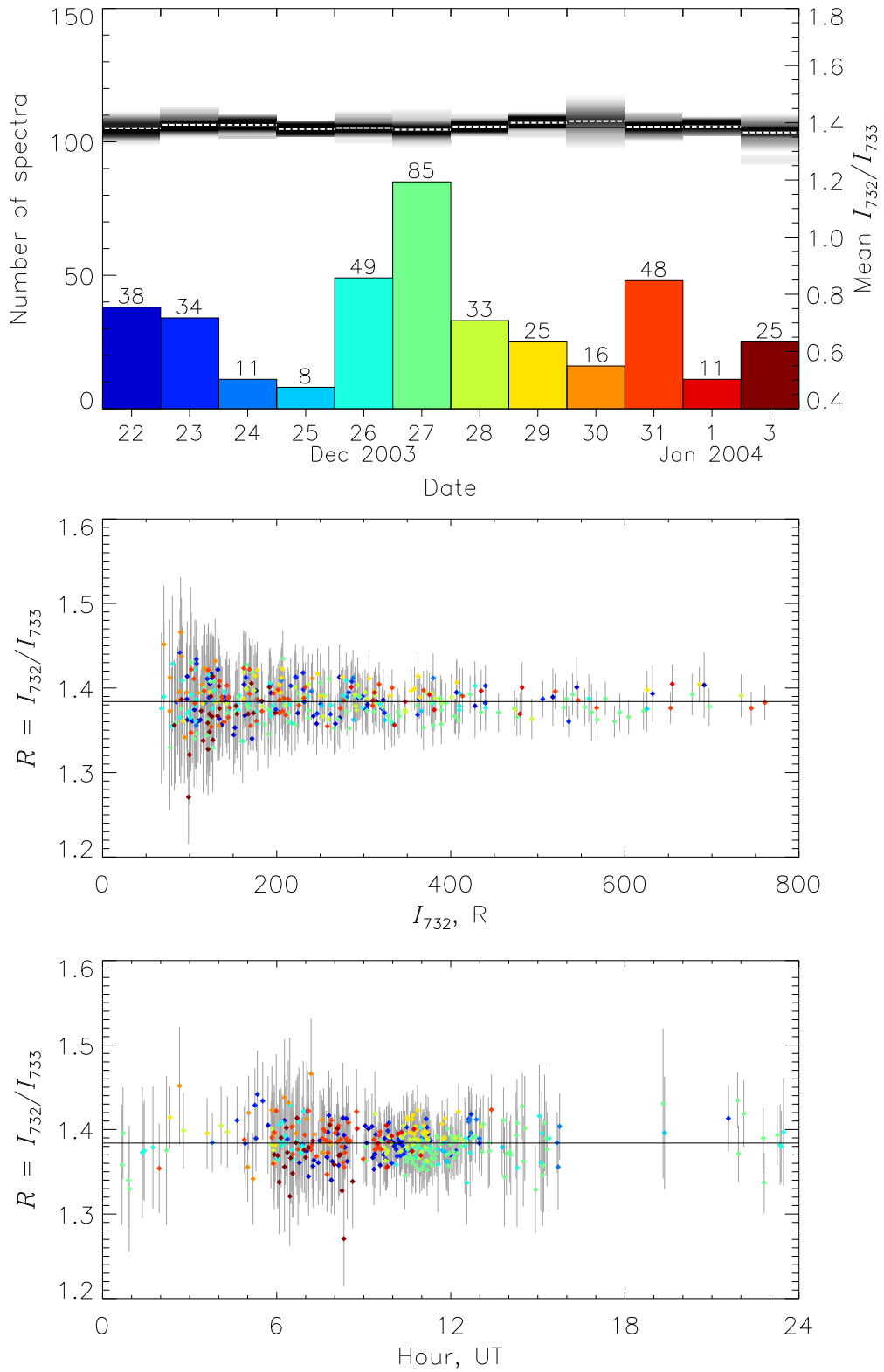


**Figure 3.** Top: histogram of spectra from the 2003–2004 season with daily distributions above; mean ratios for each day are plotted as dashed bars with values on the right axis. Middle: all spectra as a function of the $O^+$ 732.0 nm doublet brightness. Bottom: all spectra as a function of time of day (UT).

(A color version of this figure is available in the online journal.)

the wavelengths determined by Sharpee et al. (2004) and the Einstein coefficients (Zeippen 1987) for the four transitions that make up the $O^+$ doublets at 732.0 nm and 733.0 nm, which they applied, and which are used in the present work. We note that the uncertainty in the intensity measurements of Sharpee et al. (2004) means that their ratio value is comparable with our measured value.

In order to interpret auroral measurements of 732.0 nm and 733.0 nm emissions, it is necessary to understand the time evolution and various production and loss processes that control

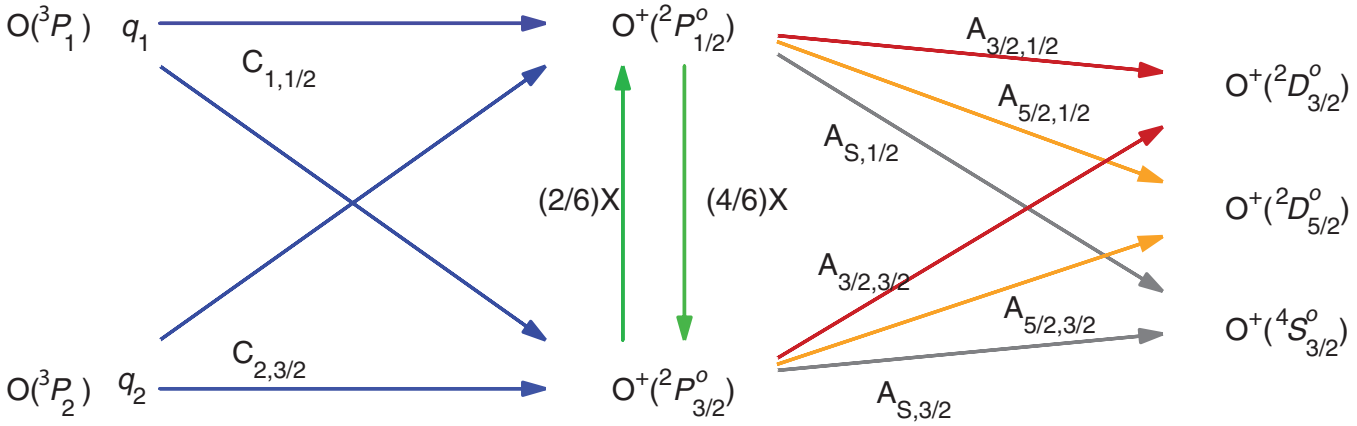


**Figure 4.** Diagram showing the production and loss processes of the two $O^+(^2P^o)$ levels (see Equations (2)–(9)).
(A color version of this figure is available in the online journal.)

the populations of each energy level. We therefore solve the continuity equations for the densities $n_{1/2}$ and $n_{3/2}$ of the two levels of $O^+(^2P^o)$, applying several variable assumptions, described below.

The densities $n_{1/2}$ and $n_{3/2}$ are given by

$$\frac{dn_{1/2}}{dt} = \eta_{1/2} - \sum_i A_{i,1/2}\, n_{1/2} - \sum_k \alpha_{k,1/2}\, n_k\, n_{1/2} + \chi_{1/2} \quad (2)$$

$$\frac{dn_{3/2}}{dt} = \eta_{3/2} - \sum_i A_{i,3/2}\, n_{3/2} - \sum_k \alpha_{k,3/2}\, n_k\, n_{3/2} + \chi_{3/2} \quad (3)$$

where $\eta_{1/2}$ and $\eta_{3/2}$ are the volume production rates to $^2P^o_{1/2}$ and $^2P^o_{3/2}$, respectively, $A_{i,1/2}$ and $A_{i,3/2}$ are the Einstein transition probabilities from $^2P^o_{1/2}$ and $^2P^o_{3/2}$, respectively, to all $i$ lower levels, $\alpha_{k,1/2}$ and $\alpha_{k,3/2}$ are the quenching rates for collision partners with density $n_k$ with the populations $n_{1/2}$ and $n_{3/2}$, respectively.

The volume production rates can be written

$$\eta_{1/2} = C_{1,1/2}\, q_1 + (1 - C_{2,3/2})\, q_2 \quad (4)$$

$$\eta_{3/2} = (1 - C_{1,1/2})\, q_1 + C_{2,3/2}\, q_2, \quad (5)$$

where $q_1$ and $q_2$ are the rates of ionization from the $O(^3P_1)$ and $O(^3P_2)$ levels, respectively, $C_{1,1/2}$ is the probability of the production of $O^+(^2P^o_{1/2})$ from $O(^3P_1)$, and $C_{2,3/2}$ is the probability of the production of $O^+(^2P^o_{3/2})$ from $O(^3P_2)$.

The final term in both Equations (2) and (3) represents thermalizing collisions that redistribute the populations between the $^2P^o_{1/2}$ and $^2P^o_{3/2}$ levels. They can be written

$$\chi_{1/2} = (2/6)\, X\, n_{3/2} - (4/6)\, X\, n_{1/2} \quad (6)$$

$$\chi_{3/2} = (4/6)\, X\, n_{1/2} - (2/6)\, X\, n_{3/2}, \quad (7)$$

where $X$ is the frequency of collisions of the ions in each level that redistribute them between the six possible states, two in $^2P^o_{1/2}$ and four in $^2P^o_{3/2}$. Figure 4 is a diagram of the production and loss terms that are included in the solutions.

Finally, the emission brightness of each doublet is given by

$$I_{732} = n_{1/2}\, A_{5/2,1/2} + n_{3/2}\, A_{5/2,3/2} \quad (8)$$

$$I_{733} = n_{1/2}\, A_{3/2,1/2} + n_{3/2}\, A_{3/2,3/2} \quad (9)$$

which are shown in Figure 4 as yellow and red arrows respectively. Thus in order to compare the measured ratio $R = I_{732}/I_{733}$ with theoretical values, it is necessary to consider the factors that may affect the densities $n_{1/2}$ and $n_{3/2}$ under auroral conditions. To this end, Equations (2)–(9) have been solved for a range of different input conditions, and the variation in $R$ examined. These conditions are as follows.

1. A range of neutral temperatures.
2. Different energy spectra of precipitating electrons.
3. A range of values of $C_{1,1/2}$ and $C_{2,3/2}$, corresponding to different production preferences of the two upper levels (i.e., deviations from statistical weights in the production).
4. Redistribution between the two upper levels from thermalizing collisions.
5. Steady state and non-equilibrium.
6. Different quenching rates for the two upper states, $\alpha_{k,1/2}$ and $\alpha_{k,3/2}$.

An input neutral atmosphere is taken from the MSIS-E-90 Atmosphere Model (Hedin 1991) for an average day during the season under study, and International Reference Ionosphere profiles are used for ionospheric input (electron density, electron and ion temperatures).

A matrix is calculated relating monoenergetic electron precipitation to height profiles of ionization, from the method described by Semeter & Kamalabadi (2005). In particular, the ionization rate profile for O is calculated for different input electron energy spectra, ranging from a high-energy Gaussian-shaped distribution, to a low-energy Maxwellian-shaped distribution. The ionization profiles are then used as input sources for the production of $O^+(^2P^o)$ calculated with ordinary differential equations for each height. The solutions are found for a range of values for "production preference" (C-factor) and "cross-state transition collision rates" (X-factor).

The modeled lifetimes of the two levels as a function of height are shown in the left panel of Figure 5. The resulting density of the two levels after 2 s, 5 s, and 40 s (steady state) are shown in the right panel of Figure 5. To estimate the effect of assuming equilibrium under auroral conditions, $R$ was determined for both steady state solutions and for short pulses, with production stopped between 0.5 and 2 s.

The steady state results are shown in Figure 6. The $R$-values have been plotted as functions of neutral temperature (at the

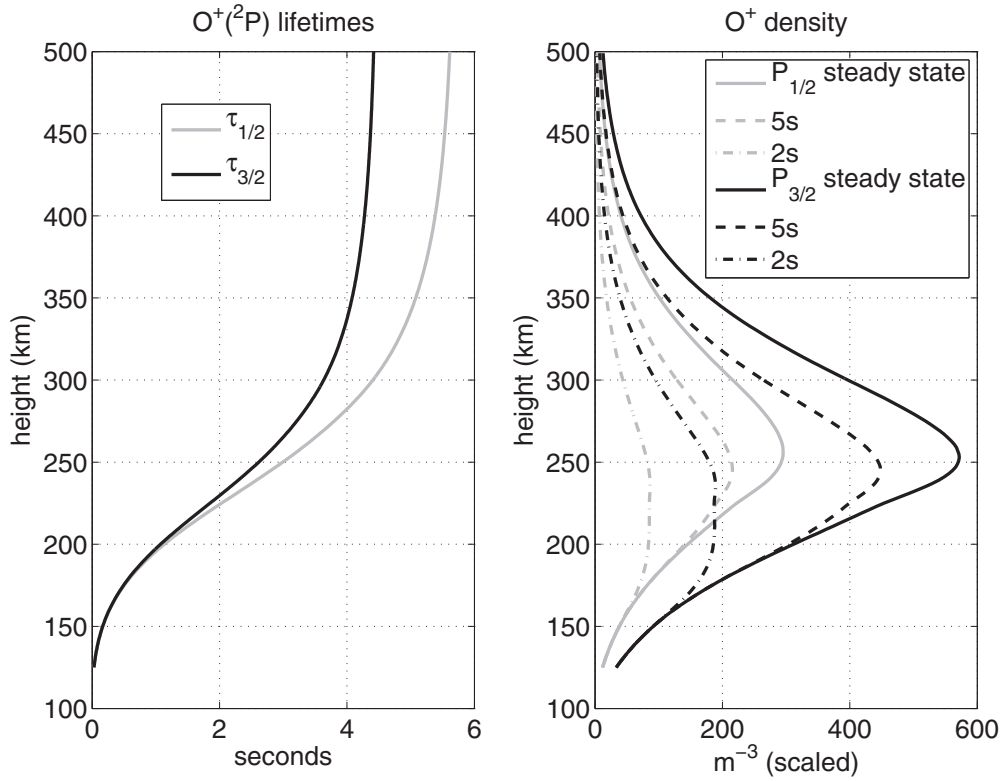


**Figure 5.** Left: height dependent lifetimes of $O^+(^2P^o)$ levels. Right: densities of both levels after 2 s, 5 s, and at steady state.

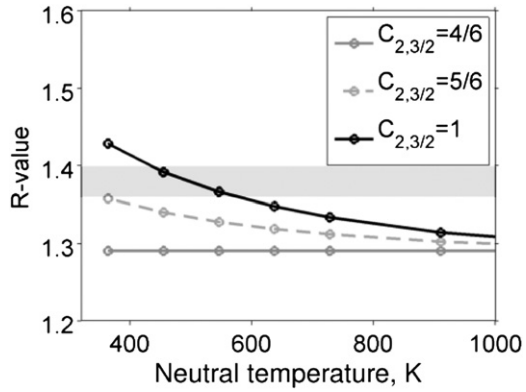


**Figure 6.** Solutions of $R$ for different production preferences ($C$-values), as a function of temperature. The measured result for $R$ is shaded in gray.

height of maximum $I_{732}$ and $I_{733}$ emission), and for extreme limits of the production preference ($C$-values), and one intermediate value. The measured value of $R = 1.38 \pm 0.02$ is shown in gray shading.

The effect of changing the input spectrum from a characteristic energy of 500 eV (as in Figure 6) to 15 keV produced an increase of less than 0.01 in the ratio values. No significant effect was found from varying the redistribution between the levels (X-factor), based on an assumption that a maximum value of this cross-level collision rate is that of the O–$O^+$ charge exchange rate (Rees 1989). The non-steady state solution increased all values of the ratio by approximately 0.01 for a short pulse lasting 2 s.

In terms of losses, there are no measurements of separate quenching rates of the two levels, $^2P^o_{1/2}$ and $^2P^o_{3/2}$, by collisions with O and $N_2$. The rates of Stephan et al. (2003) are the most recent values for quenching rates of the combined upper levels that have been used in the solutions shown. Quenching rates of Chang et al. (1993), Rees (1989), and Rusch et al. (1977) were also used, giving insignificant changes to the ratio. Although there is no evidence for separate quenching rates of the two levels, we note that by changing their ratio the value of $R$ can be increased. However, substantially different quenching rates are needed for the two levels of $O^+$ in order to match the measured ratio. The solution of the continuity equations shows that the most plausible explanation for the measured value of the ratio is that the production preference is different from statistical weights, such that the physics for auroral ionization and excitation is different from excitation in a fully ionized gas.

## 4. DISCUSSION

In the above theoretical analysis, we find that the ratio is raised when a modest change from equilibrium is assumed. However, it is not sufficient to explain our ratio values unless the production of the excited ions varies from their statistical weights. The effect on the ratio of changes in temperature also becomes significant when the C-factor is varied away from the assumption of statistical weights for the production of the ions. Temperatures of a few hundred Kelvin are very reasonable in the auroral ionosphere.

In aurorae, the emitting $O^+(^2P^o)$ is produced by electron impact ionization of O ($^3P$), which is a completely different mechanism from that present in nebulae and airglow. The impacting auroral electron has a relatively high energy ($\simeq$100 eV) and therefore forward-scattering dominates and a change in its angular momentum is unlikely; also the impacting electron is unlikely to be exchanged with an orbital electron of the O. By conservation of angular momentum, this scenario would lead to a preference for the production of $O^+(^2P^o_{1/2})$ from O ($^3P_1$) and $O^+(^2P^o_{3/2})$ from O ($^3P_2$), i.e., $C_{1,1/2} \simeq 1$ and $C_{2,3/2} \simeq 1$. This

argument was used by Sivjee et al. (1979) as a possible explanation for their ratio values. If $C_{1,1/2} \simeq C_{2,3/2} \simeq 1$, as suggested by our results and analysis, then the relative populations of $O^+(^2P^o_{1/2})$ and $O^+(^2P^o_{3/2})$ depend primarily on the relative populations of $O(^3P_1)$ and $O(^3P_2)$, and therefore on the neutral temperature. We note from the bottom panel of Figure 3 that there could be small day-to-day variations in the measured ratio (for example yellow points from December 29 lie above the mean line), which could be a consequence of small changes in neutral temperature. Simultaneous measurements of the brightness ratio and neutral temperature at about 300 km altitude over a sufficiently long period would allow a possible connection between the two to be investigated.

In considering the results of Sivjee et al. (1979), we note that they used the temperature dependent OH ratio $P_1(2)/P_1(3)$ (731.6 nm/734.1 nm) in conjunction with the measured $P_2(2)$ to correct for contamination of the 733.0 nm line by $P_2(3)$. It appears from their synthetic spectrum, convolved with their instrument function, that there was a small overlap of the 731.6 nm OH line with the 732.0 nm doublet, which has not been subtracted. It is possible that either or both of these factors may have affected their measured ratio. Their results from a single event differ significantly from our statistical results, when neither of these factors is an issue.

Any systematic error in the measurements has been estimated using a careful analysis of the spectra, using synthetic modeling, and fitting procedures. The uncertainty from the contribution of $N_2$ in the background has been minimized in this study by rejecting spectra with high background readings, and by fitting a synthetic spectrum to the band profile. Another factor is a possible small contribution from $O^+$ at 733.0 nm in the value of $\rho_1$ which would cause a small over-estimation of the ratio $R$ from Equation (1). Since our measured value of $\rho_1$ (732.9 nm/734.1 nm) of 0.368 is smaller than the theoretical value given in Phillips et al. (2004) of 0.399, we can assume that such an effect is insignificant. Using a value of $\rho_1 = 0.399$ in our calculations produces a ratio $R = 1.40 \pm 0.02$. The smallest standard deviation of $R$ is obtained for $\rho_1 = 0.373$.

## 5. CONCLUSIONS

Values of the brightness ratio $R = I_{732}/I_{733} = 1.38 \pm 0.02$ were obtained from spectrographic measurements of the two $O^+(^2D^o–^2P^o)$ doublets in low-energy aurorae for the winter season 2003–2004. This value is higher than measurements made in nebulae, and is at variance with previously reported auroral measurements of $1.55 \pm 0.05$ (Sivjee et al. 1979). In the present work, a rigorous analysis has been performed to remove the background emissions in the region of the doublets.

The ratio of the brightness of emissions from the two doublets of the $O^+(^2D^o–^2P^o)$ transitions depends on the density of ions in the excited levels of the $^2P^o$ state. These densities in turn are controlled by the processes that cause excitation, and in the case of aurorae, ionization and excitation, and the various loss processes through collisions and radiation. Solutions have been found for the continuity equations of the ions $O^+(^2P^o_{1/2,3/2})$, and the variation of the ratio determined under different assumptions. It is found that the ratio can indeed be affected by non-equilibrium conditions, by changes in the neutral temperature, by the precipitation energy distribution, and most significantly, by the production of the populations of the levels being different from the statistical weights. For a ratio approaching our measured values in low-energy aurorae it would seem that the assumption of statistical weights for the production of the two ions is the most likely one to be erroneous (in the case of low-energy aurorae $C_{2,3/2} \simeq 1$), with additional effects from non-equilibrium conditions, and variations in temperature.

To gain a better understanding of the production and loss processes responsible for the resulting densities of the two $^2P$ levels, careful measurements of the ratio should be made under different conditions, for example, in events where there could be an increase in O ionization by high-energy electron impact, and more exotic processes such as ionization by hydrogen/proton impact, and dissociative ionization (by both electrons and protons). Future work is planned to study variations of the ratio within the HiTIES data, making use of emissions at wavelengths measured in the other panels of the spectrograph mosaic filter. It will also use incoherent scatter radar measurements to study the electron temperature changes and corresponding doublet brightnesses.

We acknowledge the support of the Atmospheric Physics Group at UCL in the operation of the Spectrographic Imaging Facility and J. Sullivan, A. Stockton-Chalk, J. Holmes, and M. Dyrland in running the instruments during the winter campaign. The SIF was funded by PPARC of the United Kingdom, and is a joint project between UCL and the University of Southampton. N.I.B.J. was supported by Baghdad University while on sabbatical leave at the University of Southampton. We thank Sam Tuttle and Brendan Goodbody for their valuable assistance with programming, and Professor Tim Morris for helpful discussions on atomic physics.

## APPENDIX

## DENSITY OF THE $^2P^o_{1/2}$ AND $^2P^o_{3/2}$ LEVELS

One of the motivations of the present work is the need for accurate modeling of the emission doublet at 732.0 nm. It is one of the emissions measured by the Auroral Structure and Kinetics (ASK) instrument, which is co-located with SIF. The ASK instrument contains three narrow angle cameras all aligned with the magnetic zenith, and with different filters, one of which is centered on the 732.0 nm doublet.

Measurements of $R$ can be used to give the relative densities of the two $^2P^o$ levels, information that is needed for ionospheric modeling of emissions. From Equations (8) and (9), the ratio $R = I_{732}/I_{733}$ can be rearranged to give the ratio of the densities,

$$R_{\rm dens} = \frac{n_{1/2}}{n_{3/2}} = \frac{R\,A_{3/2,\,3/2} - A_{5/2,\,3/2}}{A_{5/2,\,1/2} - R\,A_{3/2,\,1/2}}. \quad \text{(A1)}$$

Using Einstein coefficients from Zeippen (1987) and our result, $R = 1.38 \pm 0.02$, gives a density ratio $R_{\rm dens} = 0.367 \pm 0.027$. This ratio can be used in modeling the emission brightness at 732.0 nm to compare with measurements. If the modeled total density of both levels is given by $n_{\rm tot}$, then the brightness of the 732.0 nm doublet can be found from

$$B_{732} = n_{\rm tot}\left[\frac{A_{5/2,\,1/2}\,R_{\rm dens} + A_{5/2,\,3/2}}{R_{\rm dens} + 1}\right]. \quad \text{(A2)}$$

Such results are applied in analyses of high-resolution auroral measurements, using the combination of ASK and SIF and modeling. This combination gives the distribution of energy of precipitation in time and space. It is also possible to use the lifetime of $O^+$ to measure ion velocity measurements as described in the analysis of Dahlgren et al. (2009) using the ASK instrument.

## REFERENCES


Barnett, E. W., & McKeith, C. D. 1988, MNRAS, 234, 241
Chakrabarti, S., Pallamraju, D., Baumgardner, J., & Vaillancourt, J. 2001, JGR, 106, 30337
Chang, T., Torr, D. G., Richards, P. G., & Solomon, S. C. 1993, JGR, 98, 15589
Dahlgren, H., Ivchenko, N., Lanchester, B., et al. 2009, JATP, 71, 228
Dalgarno, A., & Lejeune, G. 1971, P&SS, 19, 1653
De Robertis, M. M., Osterbrock, D. E., & McKee, C. F. 1985, ApJ, 293, 459
Hedin, A. E. 1991, JGR, 96, 1159
Ivchenko, N., Blixt, E. M., & Lanchester, B. S. 2005, GeoRL, 32, L18106
Jokiaho, O., Lanchester, B. S., Ivchenko, N., et al. 2008, AnGeo, 26, 853
Jokiaho, O., Lanchester, B. S., & Ivchenko, N. 2009, AnGeo, 27, 3465
Kaler, J. B., Aller, L. H., Epps, H. W., & Czyzak, S. J. 1976, ApJS, 31, 163
Keenan, F. P., Aller, L. H., Bell, K. L., et al. 1999, MNRAS, 304, 27
Meinel, A. B. 1950, ApJ, 111, 555
Phillips, F., Burns, G. B., French, W. J. R., et al. 2004, AnGeo, 22, 1549
Rees, M. H. 1989, Physics and Chemistry of the Upper Atmosphere (Cambridge: Cambridge Univ. Press)
Rees, M. H., Abreu, V. J., & Hays, P. B. 1982, JGR, 87, 3612
Rusch, D. W., Hays, P. B., Torr, D. G., & Walker, J. C. G. 1977, JGR, 82, 719
Seaton, M. J., & Osterbrock, D. E. 1957, ApJ, 125, 66
Semeter, J. 2003, GeoRL, 30, 1225
Semeter, J., & Kamalabadi, F. 2005, RaSc, 40, RS2006
Sharpee, B. D., Slanger, T. G., Huestis, D. L., & Cosby, P. C. 2004, ApJ, 606, 605
Sivjee, G. G., & Hamwey, R. M. 1987, JGR, 92, 4663
Sivjee, G. G., Romick, G. J., & Rees, M. H. 1979, ApJ, 229, 432
Slanger, T. G., Sharpee, B. D., Pejaković, D. A., et al. 2011, Eos Trans. AGU, 92, 291
Stephan, A. W., Meier, R. R., Dymond, K. F., Budzien, S. A., & McCoy, R. P. 2003, JGR, 108, 1034
Zeippen, C. J. 1987, A&A, 173, 410